Implementing Vibration Framework for Simulation of VIV on Rigid Pier by SPH

Hassan Ghassemi[*], Aliakbar Safaei, Shahryar Abtahi

Department of Maritime Engineering, Amirkabir University of Technology, Tehran, Iran
*Corresponding author: gasemi@aut.ac.ir

Abstract It is worth mentioning that the effect of waves on fixed and floating platforms is considered as an important element when designing any offshore structures. This paper is developed a numerical model to simulate current and wave interaction with a vertical cylinder as a platform leg using Smooth Particle Hydrodynamics (SPH) method for solving hydrodynamics part and using Finite Element Method (FEM) for structural part. SPH method is Lagrangian meshless based which is accurate enough for free surface modeling in comparison with other Eulerian mesh based methods. Capability of this method to calculate inline and cross flow forces on cylinder taking into consideration different time solution algorithms. The results showed that SPH not only creates much better result for simulating Vortex Induced Vibration (VIV) but also using the predictor-corrector algorithm for time step algorithm can leads to the most accurate results for predicting lift force.

Keywords: wave structure interaction, SPH method, predictor-corrector algorithm

Cite This Article: Hassan Ghassemi, Aliakbar Safaei, and Shahryar Abtahi, "Implementing Vibration Framework for Simulation of VIV on Rigid Pier by SPH." *American Journal of Civil Engineering and Architecture*, vol. 3, no. 4 (2015): 137-143. doi: 10.12691/ajcea-3-4-4.

1. Introduction

Construction of any massive offshore structures is usually costly therefore optimization of design of these structures is the aim of the marine engineers. In these kinds of structures due to complexity of random loading and uncertainty of environmental conditions, the risk of failure and its consequences is considerable. One of the complicated forces applied to platform leg is the in-line and cross-flow forces resulting from waves. The nature of these forces is complex and difficult to estimate properly. One of the numerical methods which have high capability in modeling the hydrodynamic phenomenon is the Smooth Particle Hydrodynamics (SPH) method. This method is a Lagrangian meshless particle base. Thus in this paper the wave structure interaction is modeled to estimate the forces on the structure using SPH method. Also, deformation of solid part has been investigated by ANSYS software. In addition, we have deployed one way couple analysis for solving solid part. In this regard, the hydrodynamic part is solved by SPH in the context of time history analysis. The calculated pressure at SPH has been imported into ANSYS software and then applied to the fluid structure interaction area. In ANSYS we have used linear elastic behavior for cylinder and the fixed support for the boundary condition. To increase the results accuracy different time algorithms were studied in this procedure to choose the best one.

Benz [1] and Monaghan [2] explained the primary developments of SPH method. It was used about 30 years ago for the first time to solve astronomy problem by Lucy [3] and Gingold and Monaghan [4]. In their model the motion of particles was simulated using the equations governing the Newtonian classic hydrodynamics. Their major achievement was to propose a method to evaluate the derivatives without using structured mesh. In SPH method, system condition is introduced with some particles which have the properties of materials and have interactions in a surrounding which is controlled by weight or smoothing functions. Monaghan and Kocharyan [5] modeled a multi-phase flow using this technique. Panizzo and Dalrymple [6] studied generated waves due to land sliding motion. Coefficient of generated waves was modeled by Gomez and Dalrymple [7] due to barrier failure collided with a high-rise building. Shao and Gotoh [8] analyzed the interaction between waves and a wall which had a gap underneath. Lee et al [9] evaluated the rising of the wave on an onshore structure using SPH method. Crespo et al. [11] developed a comprehensive computer SPH program to solve 2D and 3D flow problems.

Ostanek and Thole [12] considered several rows of short cylinders (height-to-diameter ratio¼1) in staggered configurations, where wall effects influence the vortex shedding. The dynamic interaction of slender structures with a surrounding viscous fluid represents a challenging fluid–structure interaction (FSI) problem. Increasing attention among researchers is being paid to FSI problems in many fields of engineering, from marine propulsion and vortex-induced vibrations (VIV) which is investigated by Du et al [13], Nguyen et al [14]. The suppression of VIV on flexible submerged structures has entailed a great deal

of research in the field of ocean and offshore engineering in order to ensure acceptable life spans of marine equipment, including risers, pipelines and offshore platforms (Huang, 2011 [15], Sun et al [16], Zhang et al [17]). At smaller length scales, amplification mechanisms and other engineering systems have been developed to take advantage of VIV hydrodynamics at low Reynolds numbers and harvest power from specific devices (Chen et al [18], Grouthier et al [19], Quadrante and Nishi [20], Wang et al [21]). Detailed work on the flow variability along the axis of thin cantilevers is reported in Facci and Porfiri [22]. Furthermore, several formulations have been proposed to consider the effect of parameters such as the presence of a solid wall or a free surface in the vicinity of the oscillating lamina (Grimaldi et al [23], Tafuni and Sahin [24]), the influence of the beam width-to-thickness ratio (Phan et al [25]), the coupling of two oscillating bodies in a viscous fluid (De Rosis et al [26], Intartaglia et al [27]), or the effect of a shear-dependent viscosity on the vibrations of a thin lamina (De Rosis [28]). In each case, a different hydrodynamic response is observed and a variety of hydrodynamic functions have been cast to accurately predict fluid actions in the form of added mass and damping coefficients.

2. Smooth Particle Hydrodynamics Theory

Smooth particle hydrodynamics is based on integral interpolation. Basic law indicates that any function can be estimated by the following statement [10]:

$$A(r) = \int_\Omega A(r') W(r - r', h) dr' \qquad (1)$$

In which r represents the influenced position vector, w is the weight function or Kernel function, and h is the smoothing length which adjusts the influenced zone (see Figure 1.).
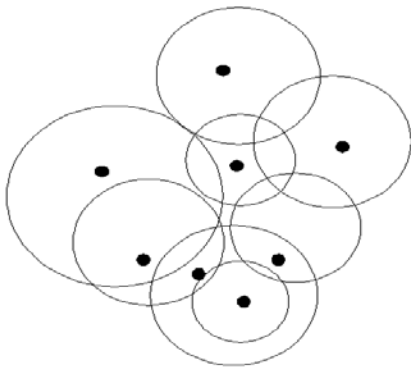
Figure 1. Influence domain of hydrodynamic particles

It is obvious that the value of h should be greater than the primary distance between particles. If equation (1) is defined discretely, then in order to have experimental estimation of particle a, it can be written:

$$A(r) = \sum m_b \frac{A_b}{\rho_b} W_{ab} \qquad (2)$$

In which m_b is the mass, ρ_b is the density and $W_{ab} = W(r_a - r_b, h)$ is the weight or Kernel function. One of the superiorities of weight function in SPH method is that derivative of weight function is achieved analytically. In

contrast in finite difference method, derivatives are calculated by neighboring points using their distances. When points are far from each other with an irregular pattern, this calculation is cumbersome. Derivative of equation 2 is evaluated as following:

$$\nabla A(r) = \sum m_b \frac{A_b}{\rho_b} \nabla W_{ab} \qquad (3)$$

Performance of smooth particle hydrodynamics model depends on the selection of Kernel function. This selection should satisfy some conditions such as positivity, normalization, uniform reduction with distance. It depends on smoothing length and dimensionless distance between particles ($q = \frac{r}{h}$), which r is the distance between a and b. Parameter h controls the area around particle affect its neighboring particles. Different smoothing functions could be applied. In this study cubic Spline smoothing functions was used as:

$$w(r, h) = \alpha_D \begin{cases} 1 - \frac{3}{2}q^2 + \frac{3}{4}q^3 & 0 \leq q \leq 1 \\ \frac{1}{4}(2 - q)^3 & 1 \leq q \leq 2 \\ 0 & q \geq 2 \end{cases} \qquad (4)$$

In this equation, α_D have different values in 2D and 3D problems.

3. Governing Equations

Basic governing equations on fluid dynamic are based on three fundamental physical rules: conservation of mass, conservation of momentum and conservation of energy. Equations of SPH motion are achieved based on Lagrangian form of these three laws. Mass conservation can be expressed as:

$$\frac{d\rho}{dt} = -\rho \nabla . V \qquad (5)$$

Equation for conservation of momentum is as following in a continuous media:

$$\frac{Dv}{Dt} = -\frac{1}{\rho} \nabla P + g + \theta \qquad (6)$$

in which v is the velocity, P is the pressure, ρ is the density, g is the gravity and θ represents the dispersion. Three forms of this statement are as artificial viscosity, laminar viscosity and turbulence model. In this study artificial viscosity proposed by Monaghan [10] was applied. According to this method equation (9) is converted to the discrete form as following:

$$\frac{dv_a}{dt} = -\sum_b m_b \left(\frac{P_a}{P_a^2} + \frac{P_b}{P_b^2} + \Pi_{ab} \right) \nabla a W_{ab} + g \qquad (7)$$

in which the pressure gradient term is as follow:

$$-\frac{1}{\rho} \nabla P = -\sum_b m_b \left(\frac{P_a}{P_a^2} + \frac{P_b}{P_b^2} \right) \nabla a W_{ab} \qquad (8)$$

The viscosity statement is defined as:

$$\Pi_{ab} = \begin{cases} \frac{-\alpha \overline{C_{ab}} \mu_{ab}}{\overline{\rho_{ab}}} & V_{ab} . r_{ab} < 0, \\ 0 & for \, other \, values \end{cases} \qquad (9)$$

in which statement of μ_{ab} and $\bar{\rho}_{ab}$ are:

$$\mu_{ab} = \frac{h v_{ab}.r_{ab}}{r_{ab}^2 + \eta^2} \qquad (10)$$

$$\bar{\rho}_{ab} = \frac{1}{2}(\rho_a + \rho_b), \bar{C}_{ab} = \frac{1}{2}(C_a + C_b); \eta^2 = 0.01\,h^2 \quad (11)$$

α is a parameter that may vary according to physical conditions of the problem. Particles move based on the hydrodynamics variance of smooth particles:

$$\bar{\rho}_{ab} = \frac{1}{2}(\rho_a + \rho_b) \qquad (12)$$

$$\frac{dr_a}{dt} = V_a + \epsilon \sum_b \frac{m_b}{\rho_{ab}} V_{ab} W_{ab} \qquad (13)$$

This method is in fact the correction speed of particle *a*. This speed can be obtained by considering the previous speed of particle *a* and also the average speed of its neighboring particles. The correction lets the particles have better establishing and for high speed of fluid particles prevents particles penetrate into each other [11].

For time discretization Beamen, Symplectic, Verlet and Predictor-Corrector time algorithms can be used. In this research these algorithms used to find the most efficient one for this physical phenomenon. The Predictor-Corrector algorithm demonstrates the variation in time interval as following:

$$\vec{v}_a^{n+\frac{1}{2}} = \vec{v}_a^n + \frac{\Delta t}{2} F_a^n;$$

$$\rho_a^{n+\frac{1}{2}} = \rho_a^n + \frac{\Delta t}{2} D_a^n; \qquad (14)$$

$$\vec{r}_a^{n+1/2} = \vec{r}_a^n + \frac{\Delta t}{2} \vec{V}_a^n$$

Value of $P_a^{n+1/2} = f\left(\rho_a^{n+\frac{1}{2}}\right)$ is then calculated using equation of state. These values will be modified according to the forces in the middle time step:

$$\vec{v}_a^{n+1/2} = \vec{v}_a^n + \frac{\Delta t}{2} F_a^{n+1/2};$$

$$\rho_a^{n+1/2} = \rho_a^n + \frac{\Delta t}{2} D_a^{n+1/2}; \qquad (15)$$

$$\vec{r}_a^{n+1/2} = \vec{r}_a^n + \frac{\Delta t}{2} \vec{V}_a^{n+1/2}$$

Finally values at the end of the time step will be calculated as follow:

$$\vec{v}_a^{n+1} = 2\vec{v}_a^{n+1/2} - \vec{v}_a^n;$$

$$\rho_a^{n+1} = 2\rho_a^{n+\frac{1}{2}} - \rho_a^n; \qquad (16)$$

$$\vec{r}_a^{n+1} = 2\vec{r}_a^{n+1/2} - \vec{r}_a^n$$

Pressure value will also be evaluated by using density values and based on $P_a^{n+1} = f(\rho_a^{n+1})$.

4. Wave Generation

Generated waves were derived from the first order theory using Piston wave maker. The displacement of paddle can be obtained as [13]:

$$X_p(t) = \frac{H}{k}\left[\tanh\big(X(t)\big) + \tanh\left(\frac{k}{d}\lambda\right)\right];$$

$$X(t) = \frac{k}{d}\big(ct - X_p(t) - \lambda\big) \qquad (17)$$

In which X_p is paddle displacement, d is water depth, H is the wave height, $k = \sqrt{(\frac{3H}{4d})}$ is the wave number, λ is wave length and $c = \sqrt{g(d+H)}$ is the speed.

The speed of wave-generated motion is obtained from the following relation [13]:

$$u_p(t) = \frac{cH}{d} \cdot \frac{1}{\cos h^2 X(t) + \frac{H}{d}} \qquad (18)$$

where u_p is paddle displacement velocity.

5. Porous Coefficient

One of the important factors for deformation of cylinder due to vortex and wave force depends on porosity of the cylinder. The porous media model can be used for a wide variety of single phase and multiphase problems, including flow through packed beds, filter papers, perforated plates, flow distributors, and tube banks. When you use this model, you define a cell zone in which the porous media model is applied and the pressure loss in the flow is determined via your inputs as described in Momentum Equations for Porous Media.

5.1. Momentum Equations for Porous Media

The porous media models for single phase flows and multiphase flows use the Superficial Velocity Porous Formulation as the default. ANSYS calculates the superficial phase or mixture velocities based on the volumetric flow rate in a porous region. The porous media model is described in the following sections for single phase flow, however, it is important to note the following for multiphase flow:

- In the Eulerian multiphase model (Eulerian Model Theory in the Theory Guide), the general porous media modeling approach, physical laws, and equations described below are applied to the corresponding phase for mass continuity, momentum, energy, and all the other scalar equations.
- The Superficial Velocity Porous Formulation generally gives good representations of the bulk pressure loss through a porous region. However, since the superficial velocity values within a porous region remain the same as those outside the porous region, it cannot predict the velocity increase in porous zones and therefore limits the accuracy of the model.

Porous media are modeled by the addition of a momentum source term to the standard fluid flow equations. The source term is composed of two parts: a viscous loss term (Darcy, the first term on the right-hand side of Equation 19, and an inertial loss term (the second term on the right-hand side of Equation 19)

$$S_i = -\left(\sum_{j=1}^{3} D_{ij}\mu v_j + \sum_{j=1}^{3} C_{ij}\frac{1}{2}\rho|v|v_j\right); \qquad (19)$$

Where Si is the source term for the i th (x, y, or z) momentum equation, Asb(v) is the magnitude of the velocity and D and C are prescribed matrices. This momentum sink contributes to the pressure gradient in the porous cell, creating a pressure drop that is proportional to the fluid velocity (or velocity squared) in the cell. To recover the case of simple homogeneous porous media:

$$S_i = -\left(\frac{\mu}{\alpha}v_i + C_2\frac{1}{2}\rho|v|v_i\right) \tag{20}$$

Where alpha is the permeability and C_2 is the inertial resistance factor, simply specify D and C as diagonal matrices with $1/\alpha$ and C_2, respectively, on the diagonals (and zero for the other elements). ANSYS FLUENT [29] also allows the source term to be modeled as a power law of the velocity magnitude:

$$S_i = -C_0 |v|^{C_1} = -C_0 |v|^{(C_1-1)} v_i \tag{21}$$

where C_0 and C_1 are user-defined empirical coefficients.

6. Results and Discussions

The schematic modeling and the diminutions are presented in Table 1 and Figure 2. The piston type wave-maker is in the left side of the tank and vertical cylinder is in the middle of calculation range.
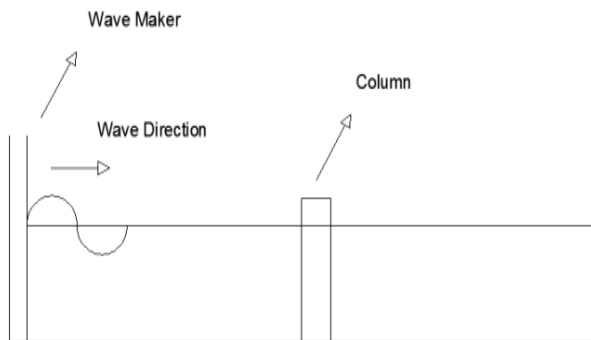
Figure 2. Study domain

Table 1. Computational Domain

Parameters	Values
Cylinder Diameter	D
Reynolds Number	Different
Channel Width	5D
Channel Length	10D
Height of Channel	5D
Strouhal Number	0.13
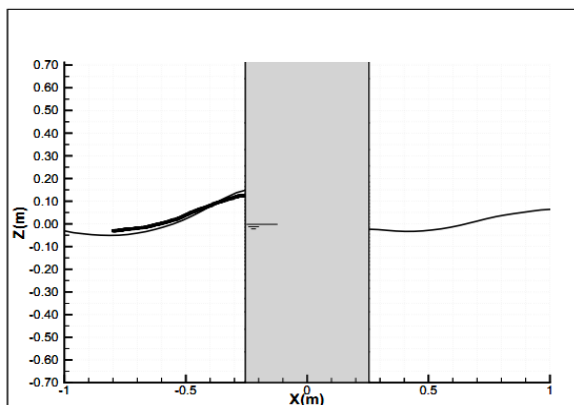
Figure 3. Geometry of the problem

Here the interaction of waves with fixed vertical cylinder is studied with regular waves. The waves generated in a range of $L/D = 5$ in which L is the wave length and D is the cylinder diameter selected as 0.508 m. The geometry of the problem is shown in Figure 3.

To evaluate wave in-line and cross-flow forces on the cylinder, Keulegan-Carpenter number was assumed to be 3.14. Using this geometry the number of particles in this problem was 585000. In addition, the total analysis time was selected as 50 seconds. All problems were solved using a personal computer with 16 Giga-bytes memory. This computer had a-four-cell processor of 3.4 Hz power each. It should be noted that the developed code was a serial one so the consuming time to solve the problem was between 300 to 320 hrs with respect to the time algorithm which was used. Concerning the mentioned problem, necessity of using parallel codes is obvious. Even using the super-computers to save time seems to be logical.
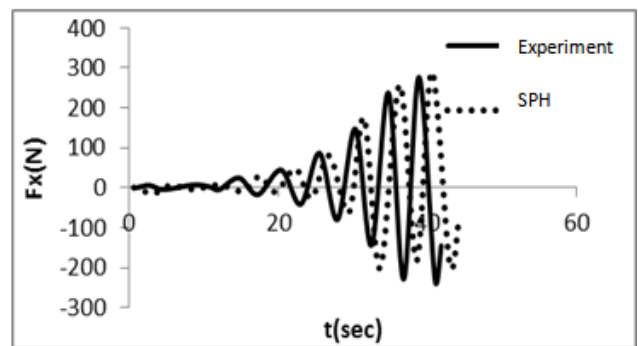
Figure 4. Wave induced Lift force using the Beamen time algorithm
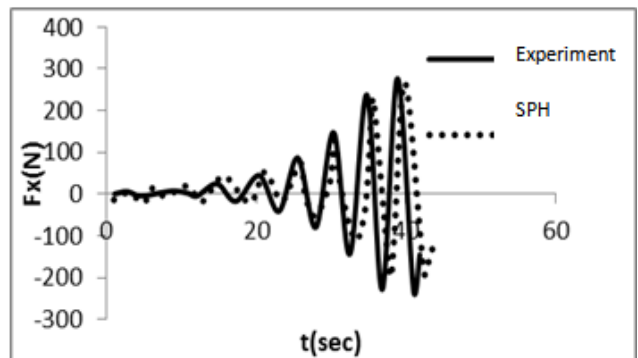
Figure 5. Wave induced Lift force using the Symplectic time algorithm
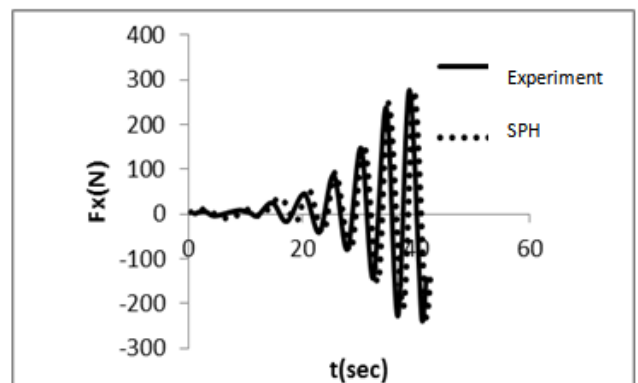
Figure 6. Wave induced Lift force using the Verlet time algorithm

Figure 4 to Figure 7 show the total wave induced fluctuating forces (Lift) on the cylinder in time domain,

using different time algorithms i.e. Beamen, Symplectic, Verlet and predictor-corrector where is compared to Sangita [30]. It can be seen that some of these time algorithms demonstrate discrepancies both in amplitude and phase. For each of them the average calculated error is shown in Table 2.
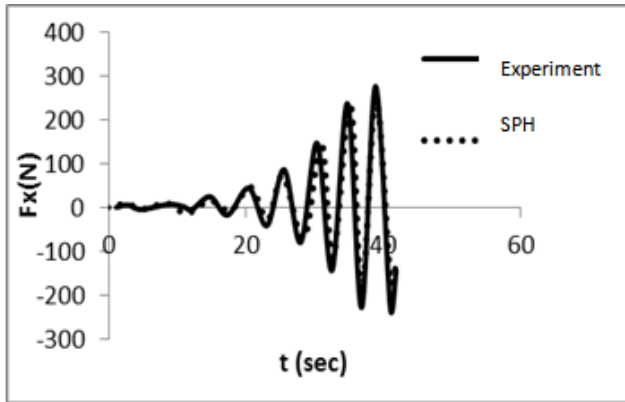
Figure 7. Wave induced Lift force using the predictor-corrector time algorithm

Table 2. Average calculated error for time algorithm

Algorithm of Time Solution	Value of Average error (%)
Beamen	9.93
Symplectic	5.68
Verlet	3.25
Predictor-Corrector	1.08
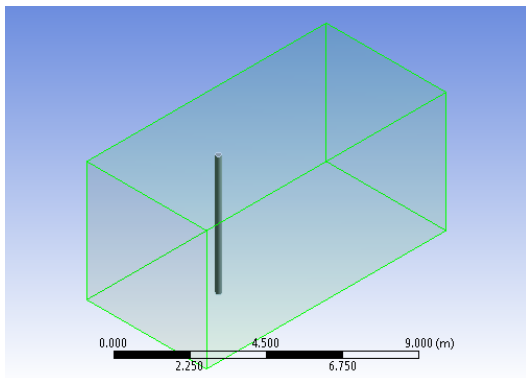
Figure 8. Computational domain
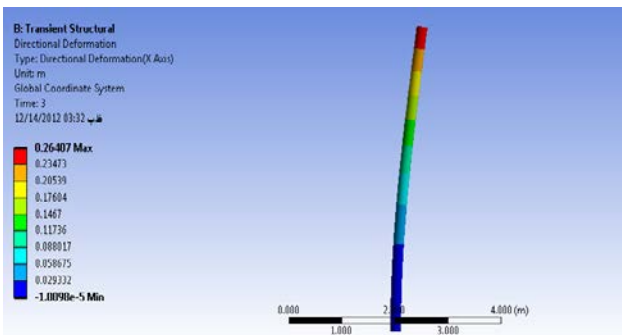
Figure 9. Deformation of cylinder due to vortex shedding by ANSYS

As it can be seen, predictor-corrector time algorithm has the minimum computational error in this problem. Its computational time was 318 hours and 20 min for the above problem with 585000 particles. Computational domain is shown in Figure 8. After extracting pressure

distribution on cylinder by the aid of ANSYS the deformation of cylinder have been investigated. In Figure 9 and Figure 10 the deformation and shear stress of cylinder due to the vortex shedding has been shown, respectively.

Figure 11 to Figure 14 respectively shows the lift coefficient time history for current where Reynolds number is 50000, lift coefficient time history for current where Reynolds number is 100000, computed force due to imported pressure on cylinder in different Reynolds number and also effect of porosity on computed forces.
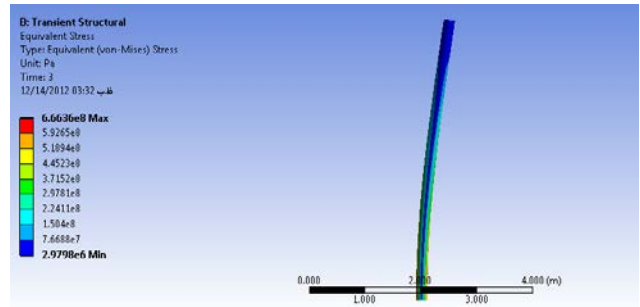
Figure 10. Shear Stress of cylinder due to vortex shedding by ANSYS
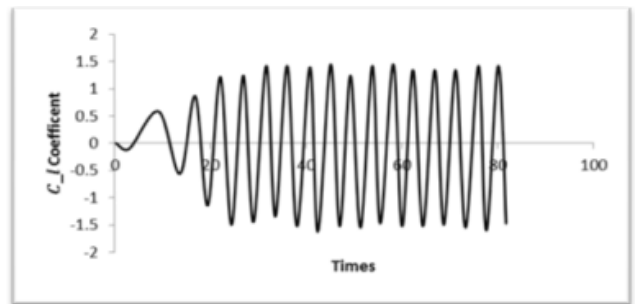
Figure 11. Lift Coefficient for Reynolds 50000
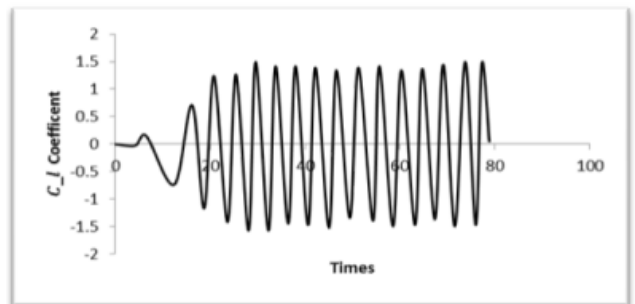
Figure 12. Lift Coefficient for Reynolds 100000

Table 3. Inlet Current Conditions

Reynolds	Inlet Velocity	State
214	0.00214	1
10000	0.1	2
50000	0.5	3
100000	1	4

7. Conclusions

In this research a wave collision to the platform bases was modeled using smooth particle hydrodynamics method. In section two, governing equations on smooth

particle hydrodynamics method was considered and the way of solving the problem is defined. For different situations, different boundary conditions were used. After defining the problem and the procedure of solving the Navier-Stokes equations by smooth particle hydrodynamics method, in the next section modeling of wave interaction with platform bases was done. In the numerical modeling four time-algorithms were used and each of them was compared with the experimental results. As it was noticed Predictor-Corrector algorithm had more accuracy and also higher computational cost in comparison with other time algorithms. Additionally by increase of Reynolds number, lift force around the riser or column was increased. Furthermore by changing flow regime from turbulent to laminar, vortex shedding became more regular and lift force was decreased consequently the problem is highly affected by Reynolds number. Finally porous coefficient has a reverse relation with lift force and by increasing porous coefficient, lift force was diminished because porous media will dissipate vortexes by making it divergent. Also in the procedure of solving, due to the high cost of computation, using the parallel codes seems necessary to accelerate the time process
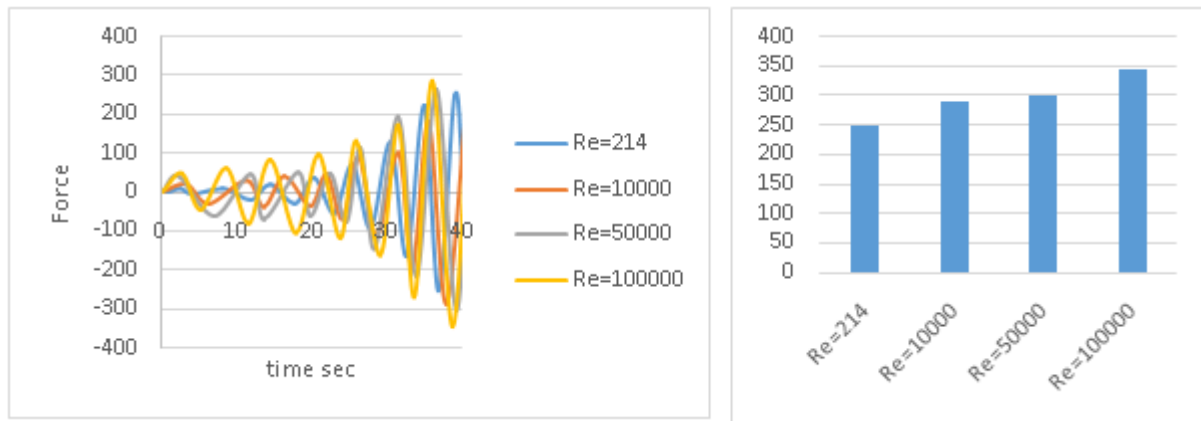
Figure 13. Computed Lift Forces on Column in different reynolds
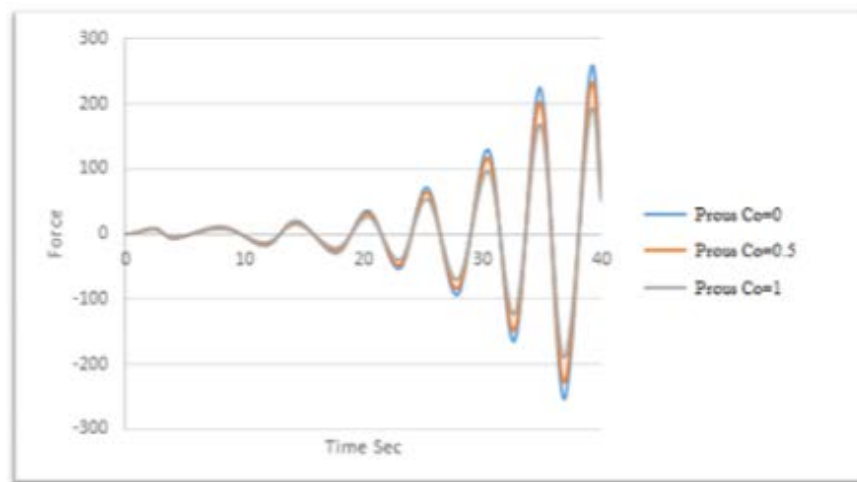
Figure 14. Force in different Porous Coefficient

References

[1] Smooth particle hydrodynamics: a review. Benz, W. In J.R. Buchler, editor, The Numerical Modeling of Nonlinear Stellar Pulsatations, pp. 269-288.Kluwer Academic Publishers, 1990. Cited in: Campbell, J.

[2] Monaghan J. J .Siam, (1982), Why particle methods work. J. on Scientific and Statistical Computing, Vol 3(4), pp422-433.

[3] Lucy, LB., Astron J.(1977), A numerical approach to the testing of the fission hypothesis, Astronomical Journal, vol. 82, Dec. 1977, p. 1013-1024.

[4] Gingold, RA., Monaghan, J., Mon Not R Astron Soc,(1977) Smoothed particle hydrodynamics—theory and application to non-spherical stars, Vol.181, pp:375-389.

[5] Monaghan, J. J. and Kocharyan,(1995) A SPH simulation of multi-phase flow, Computer Physics Communication, Vol.87, pp: 225-235.

[6] Panizzo, A. and Dalrymple, R. A.,(2004), "SPH modeling of underwater landslide generated waves" In Proc. 29th International Conference on Coastal Engineering, pp: 1147-1159.

[7] Gomez-Gesteira, M. and Dalrymple, R. A., (2004), "Using a 3D SPH Method for Wave Impact on a Tall Structure", J. Waterway, Port, Coastal and Ocean Engineering, Vol. 130(2), pp: 63-69.

[8] Shao, S. and Gotoh, H.,(2004) "Simulating coupled motion of progressive wave and floating curtain wall by SPH-LES model", Coastal Engineering Journal, Vol. 46(2), pp: 171-202.

[9] Lee, E.S., Violeau, D., Benoit, M., Issa, R., Laurence, D., and Stansby, P.(2006), "Prediction of wave overtopping on coastal structures by using extended Boussinesq and SPH models", In Proc. 30th International Conference on Coastal Engineering, pp: 4727-4740.

[10] G R. Liu and M B. Liu., (2002). "Smooth Particle Hydrodynamic a mesh free particle method" World scientific publishing Co. Pte .Ltd. ISBN 981-238-456-1.

[11] Crespo, A., (2008). "Application of the smoothed particle hydrodynamics model SPHysics to free surface hydrodynamics", Ph.D. thesis, University of De Vigo.

[12] Ostanek, J.K., Thole, K.A., 2012. Wake development in staggered short cylinder arrays within a channel. Exp. Fluids 53, 673-697.

[13] Du, L., Jing, X., Sun, X., 2014. Modes of vortex formation and transition to three-dimensionalityin the wake of a freely vibrating cylinder. Journal o f Fluids and Structures 4 9, 554-573.

[14] Nguyen, T., Koide, M., Yamada, S., Takahashi, T., Shirakashi, M., 2012. Influence of mass anddamping ratios on VIVs of a cylinder with a downstream counterpart in cruciform arrangement. Journal of Fluids and Structures 28, 40-55.

[15] Huang, S., 2011. VIV suppression of a two-degree-of-freedom circular cylinder and dragreduction of a fixed circular cylinder by the use of helical grooves. Journal of Fluids and Structures 27, 1124-1133.

[16] Sun, L., Zong, Z., Dong, J., Dong, G.H., Liu, C., 2012. Stripwise discrete vortex method for VIV analysis of flexible risers. Journal of Fluids and Structures 35,21-49.

[17] Zhang, H., Fan, B., Chen, Z., Li, H., 2014. Numerical study of the suppression mechanism of vortex-induced vibration by symmetric Lorentz forces. Journal of Fluids and Structures 4 8, 62-80.

[18] Chen, X., Xu, S., Yao, N., Shi, Y., 2010. 1.6 V Nanogenerator for mechanical energy harvesting using PZT nanofibers. Nano Letters 10, 2133-2137.

[19] Grouthier, C., Michelin, S., Bourguet, R., Modarres-Sadeghi, Y., De Langre, E., 2014. On the efficiency of energy harvesting using vortex-induced vibrations of cables. Journal of Fluids and Structures 49, 427-4 40.

[20] Quadrante, L.A .R., Nishi, Y., 2014. Amplification/suppression of flow-induced motions of an elastically mounted circular cylinder by attaching tripping wires. Journal of Fluids and Structures 48, 93-102.

[21] Wang, J., Ran, J., Zhang, Z., 2014. Energy harvester based on the synchronization phenomenon of a circular cylinder. Mathematical Problems in Engine erring 2014, 1-9.

[22] Facci, A .L., Porfiri, M., 2013. Analysis of three-dimensional effects in oscillating cantilevers immersed in viscous fluids. Journal of Fluids and Structures 38,205-222.

[23] Grimaldi, E., Porfiri, M., Soria, L., 2012. Finite amplitude vibrations of a sharp-edged beam immersed in a viscous fluid near a solid surface. Journal of Applied Physics 112, 104 907.

[24] Tafuni, A., Sahin, I., 2013. Hydrodynamic loads on vibrating cantilevers under a free surface in viscous fluids with SPH. In: Proceedings of the ASME 2 013International Mechanical Engineering Congress and Exposition (IMECE 2013), IMECE2013 63792.

[25] Phan, C.N., Aureli, M., Porfiri, M., 2013. Finite amplitude vibrations of cantilevers of rectangular cross sections in viscous fluids. Journal of Fluids and Structures 40, 52-69.

[26] De Rosis, A., 2014. Harmonic oscillations of laminae in non-Newtonian fluids: a lattice Boltzmann-Immersed Boundary approach. Advances in Water Resources 73, 97-107.

[27] Intartaglia, C., Soria, L., Porfiri, M., 2014. Hydrodynamic coupling of two sharp-edged beams vibrating in a viscous fluid. Proceedings of the Royal Society of London: Mathematical, Physical and Engineering Sciences Series A 470, 20130397.

[28] De Rosis, A., 2014. Harmonic oscillations of laminate in non-Newtonian fluids: a lattice Boltzmann-Immersed Boundary approach. Advances in Water Resources 73, 97-107.

[29] ANSYS USER MANUA, 2014.

[30] Sangita,M. Computation of Solitary Waves During Propagation and Run up on a Slope. J. Ocean Engineering, Volume 26, Issue 11, Pages 1063-1083, November 1999.